Scan vs. BIM: Patch-based construction progress monitoring using BIM and 3D laser scanning (ProgressPatch)

Felix GRUNER, Enrico ROMANSCHEK, Daniel WUJANZ and Christian CLEMEN, Germany

Key words: Laser scanning, Building Information Modeling (BIM), Construction progress monitoring, Change detection

SUMMARY

This paper presents a new method and experimental software for automated construction progress monitoring. The algorithm is based on an as-planned Building Information Model (BIM) which is compared with the 3D point clouds from a static Terrestrial Laser Scanner (TLS). The point clouds are measured on-site during the construction process. Due to the to the efficient combination of measurement and model, the construction work can be carried out more quickly and with fewer defects.
A vital prerequisite for construction progress monitoring is the co-registration of the acquired data. If this step in the processing chain is biased, all computed deviations among BIM and captured data will consequently be erroneous - false conclusions are inevitable.
In contrast to other solutions our approach is plane-based for both, the point cloud and the building model. The reason why planes are used instead of points can be justified by the large amount of data is reduced to plane parameters, which drastically reduces the required data volume. The small plane sections used for this purpose are called patches. The presented method considers the error budget of the scanner, its calibration and registration by variance propagation utilizing stochastic tests. The building model is reduced to component surfaces called faces. Construction progress is derived through a comprehensive comparison of patches to faces. The position of the laser scanner in the scene is also used, which gives additional information on the visibility and orientation of the building components. The basis of the method are detected patches in the recorded point clouds as well as planned building faces that need to be transformed into an identical reference coordinate system. Therefore, a new method for the co-registration of point clouds into a BIM-coordinate system was developed, whereby the co-registration directly extracts planes from the building model. The new methods are validated within an actual construction project where three successive construction phases were monitored.

Scan vs. BIM: Patch-based construction progress monitoring using BIM and 3D laser scanning (ProgressPatch)

Felix GRUNER, Enrico ROMANSCHEK, Daniel WUJANZ and Christian CLEMEN, Germany

1. INTRODUCTION

A new method for automated construction progress monitoring using faces from a building model and patches from laser scanning data (scan vs. BIM) is presented. In contrast to other solutions the approach is plane-based. Deploying local plane parameters reduces the original data volume of the point clouds and increases the detection accuracy since adjusted plane parameters are more accurate than single points. In the presented test case, the data volume decreases from 4.3 GB to 43.4 MB. Since the majority of buildings have planar surfaces, this geometric representation is considered to be suitable for construction progress monitoring. The general idea to use extracted planes instead of points from laser scans was presumably introduced by Gielsdorf et al. 2004 in the context of TLS calibration. Later contributions of the same research group added a first implementation of plane-to-plane registration (Rietdorf 2005) that finally lead to *Scantra* (Wujanz et al. 2018), a commercial software that was used in this contribution. It is well known that the error budget of scanner, calibration and registration have an immediate impact onto the outcome of monitoring. Thus, all aforementioned error sources are considered within a stochastic model. This stochastic model is used for both, the registration of scans and scan vs. BIM progress monitoring, where the latter represents the focus of this paper. The presented approach utilizes statistical hypothesis tests to check if the deviation between as-built and as-planned is significant or not. After this check, the confidence interval and the tolerance interval are compared, in order to verify if a significant deviation is structurally acceptable or not. The comparison can be used to check an object´s existence, orthogonal distances and rotations of building components, by assigning properties to each face F_i

1. visible $\boldsymbol{v}: \mathbf{F} \rightarrow$ {visible, not visible}
2. measured $\boldsymbol{m}: \mathbf{F} \rightarrow$ {measured, not measured, unknown}
3. permanence $\boldsymbol{o}: \mathbf{F}(\boldsymbol{v}, \boldsymbol{m}) \rightarrow$ {existent, absent, unknown}
4. shift $\boldsymbol{s}: F_v \rightarrow$ {no, significant, uncertain}, {in tolerance, off tolerance, uncertain}
5. rotation $\boldsymbol{r}: F_v \rightarrow$ {no, significant, uncertain}, {in tolerance, off tolerance, uncertain}

The first two properties $\boldsymbol{v}$ and $\boldsymbol{m}$ are used to detect the presence $\boldsymbol{o}$ or absence of an object. The attributes $\boldsymbol{s}$ and $\boldsymbol{r}$ specify a component as being in the correct position or detects a parallel displacement or erroneous rotations of visible faces $\mathbf{F_v}$.
The detailed results of the fully automatic analysis are written to a detailed protocol and relevant parameters are attached directly to the building components objects in the BIM Software and maybe exported as Industry Foundation Classes (IFC) property sets. In this way, it is possible

to detect deviations of the actual construction process from the planned construction process at an early stage and thus prevent delays and cost overruns. If construction errors occur, the originator can be identified and defect management can be carried out directly on the BIM model.

A prerequisite for the comparison of scans captured on a construction site and a BIM is that both data sources are transformed into an identical reference coordinate system. With the used plane-based registration software it is now possible to export faces from the BIM model and use their planes for co-referencing the point cloud to the BIM. This eliminates the need for control points in the reference coordinate system, which is one of the major practical advantages of the presented method. The answer to the following questions will be calculated by the presented algorithm:

- Was the face potentially visible from a scanner position?
- Was the face actually measured from a scanner position?
- How accurately are the scan-patches on the BIM-face measured?
- Is the deviation significantly larger than a given tolerance?

To answer these questions, the precision and accuracy of both, patches and registration are considered. The presented approach is based on a stochastic model and variance propagation.

2. Related Research

The presented research is related to both, construction monitoring and the comparison of as-built versus as-planned models. Hence, both subjects are discussed in sections 1 and 2.2.

2.1. Construction Progress Monitoring

Omar and Nehdi 2016 examined and compared different technologies of automated and electronic building data. Figure 1 illustrates the main categories into which the approaches can be divided.

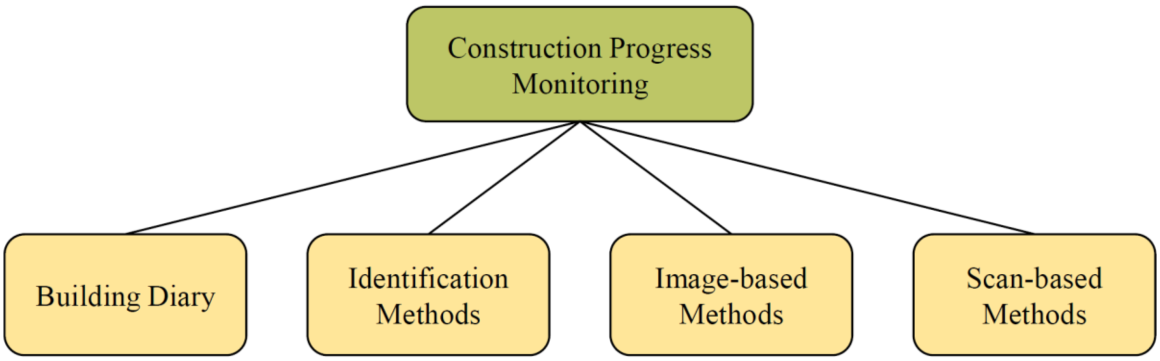

Figure 1: Overview of different methods of documenting the construction progress (based on Omar and Nehdi 2016)

The most common method for documenting the progress of construction in practice is the building diary. A construction diary should record the status and progress of the construction work as well as all noteworthy events during the construction process. Scott and Assadi 1997 already showed the limitations of analogue construction diaries and how these disadvantages can be eliminated with the help of digital documentation. Further developments are moving in the direction of mobile recording with the help of smartphones and tablets (Bermudez 2012). The apps available for this can associate photos and comments to the planning data.

RFID transponders in and on building components are used in construction industry because they enable unambiguous identification. However, information on differences in position and shape of individual components cannot be retrieved with RFID. It is becoming established for many applications in construction and Valero and Adán 2016 give a review of these technologies that have recently been integrated with RFID.

Image-based methods can be divided into two approaches. In the first approach, information is extracted by image processing operators. In the other approach, a point cloud can be calculated from the imagery, with which further work is done, such as in Tuttas et al. 2017. One of the possibilities is to compare the real image of the as-built state with a synthetic image generated from the model. Based on this idea, Rebolj et al. 2008 present a concept for automated construction progress control. Furthermore, it is possible to project the construction model into the images of fixed cameras in order to compare the as-built with the as-planned state. This method is based on changes in intensity values. A disadvantage of this approach is that the changes are often not due to actual construction progress, but have other causes, such as personnel or stored construction material. (Ibrahim et al. 2009). A detailed, comprehensive comparison of image-based systems that also make use of time-lapse image sequences or videos is provided by Yang et al. 2015.

The last option specified here is scanning with active sensors to generate point clouds. As the density of data in point clouds is very high and processing can be carried out in different ways, Xu and Stilla 2021 give a thorough overview of the acquisition and processing techniques for building reconstruction, also with regard to monitoring the construction progress. Bassier et al. 2019 also integrate a BIM model to quantify the progress and quality of the construction process. An attempt is made to determine the condition of components based on a trained classification of concrete walls using machine learning. In contrast, Bosché et al. 2015 are particularly considering the case of tracking components with circular cross-sections, which essentially include pipes, conduits and ducts. In the infrastructure sector, Puri and Turkan 2020 monitored the construction progress of a bridge with the help of mobile laser scanning.

2.2. Comparison as-planned and as-built status

Most approaches for comparing target geometries and point clouds are based on checking geometric deviations. The ICP algorithm by Besl and McKay 1992 plays a major role here. It can be used for registration or for the comparison of point clouds. In order to carry out the comparison to a model, the building model must either be transferred into a point cloud by sampling, as in Guo et al. 2020, or the shortest distance to a model surface is searched for instead of the nearest point. The disadvantage of the ICP algorithm is its proneness to outliers (Wujanz 2012). It is therefore unsuitable for real construction sites, as building materials are temporarily stored on the site and a large number of auxiliary constructions are used. If scan points are assigned to wrong component surfaces, an invalid result can be generated. This becomes especially clear when the scan points are colored depending on the previously calculated distance. Edges of components then usually appear correct, although the component is not present at all. This problem is avoided by using an overlap threshold value when comparing target surfaces and actual surfaces.

This is also used in a similar way in Bosché 2010. The threshold value also determines whether a component has been built or not. In Rebolj et al. 2017, the quality of point clouds is analyzed and related to the derivation of BIM elements for determining the construction progress.

A different approach is used in Stilla and Xu 2023, where a voxel grid is placed over the entire scene and the occupancy is determined. The change can be determined from different epochs and by using BIM models.

3. METHODOLOGY

The analysis can be divided into six steps as portrayed in Figure 2:

1. The point clouds for each station are relatively registered and then co-registered into the BIM coordinate reference system using identical planes.
2. The scan vs. BIM situation is evaluated concerning the visibility of every face in $\mathbf{F}$ from every scan station in S in order to find all $\mathbf{F_v}$.
3. Having the BIM Faces $\mathbf{F_v}$ and the TLS patches $\mathbf{P}$ available in the same coordinate reference system, the faces and patches are logically assigned based on geometric proximity in step.
4. After that, a statistical test is carried out to determine whether the accuracy is sufficient for an evaluation in step.
5. If this is the case, the calculated distance is classified in a tolerance interval.
6. The results are exported and visualized as text-protocol and properties of building components in the BIM software.

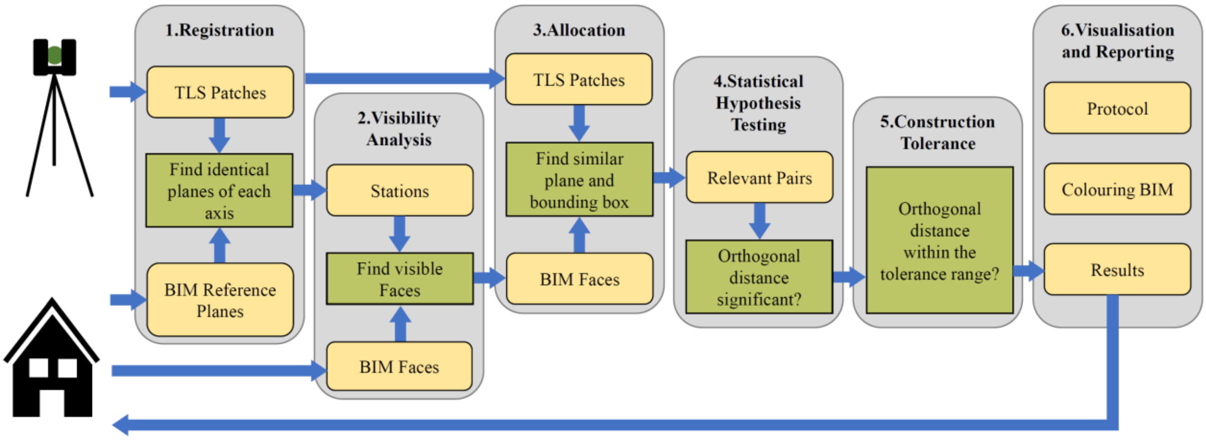

Figure 2: Workflow of the new scan vs. BIM approach

For some parts formulas are shown, in order to understand them better, a fixed notation of formula signs is used. The main attributes are explained in Table 1.

Table 1: Description of the notation used in this research paper

attribute	meaning
S	stations $\mathbf{S_i}$ of an epoch **S** $\rightarrow$ $(t_x, t_y, t_z, q_0, q_1, q_2, q_3, C_{XX}^S)$
F	faces $\mathbf{F_i}$ from BIM of an epoch **S** $\rightarrow$ $(c_x, c_y, c_z, n_x, n_y, n_z, \text{Polygon})$
$\mathbf{F_V}$	visible faces $\mathbf{F_{V_i}}, \mathbf{F_V} \subset \mathbf{F}$
$\mathbf{P^{LOC}}, \mathbf{P^{BIM}}$	set of all patches $\mathbf{P_i}$ from TLS of an epoch in the local (LOC) and the desired building coordinate reference system (BIM)
O	octants $\mathbf{O_i}$ divide space around station into octants
o	target value object permanence
p	target value position
a	distance between patch and face
$\boldsymbol{\sigma_a}$	standard deviation of the distance
$\mathbf{C_{XX}}$	covariance matrix from the plane-based registration software

The plane-based registration software uses a database to store the detected planes, which are referred to as patches in this context. A patch is an enclosed part of a plane. The patch detection depends on 3 parameters:

1. Maximum number of detected planes per station
2. Limit value for planarity: standard deviation for the planarity of a plane
3. Minimum number of points per plane

In addition, all calculations and results of the registration are stored in the database. The two data sources are used at the beginning to write faces from BIM and patches from TLS into a uniformly structured CSV file. The data is divided into two related files, the first containing the faces from BIM or patches from TLS. The second one describes the plane of the face or the patch.

- Face/Patch = {StateId, ObjectGuid, FaceId, PlaneId, BBox, Polygon}
- Plane = {PlaneId, Normal, Position, PlaneX, C_{XX}}

The **StateId** consists of a **CreateStateId** and a **DemolishedStateId**. This combination makes it possible to determine whether a face was already present in the existing building and/or was demolished, or whether it is newly planned and will be added during construction. The component is uniquely named by a **ObjectGuid** and the individual faces of a component are differentiated by the **FaceId**. A plane is assigned via a **PlaneId**. In addition, the first file contains the smallest two-dimensional bounding box and the two-dimensional polygon.
The second part includes the face normal $\vec{\mathbf{n}}$ and a point located on the plane as a position. **PlaneX** indicates the direction of the local x-axis, because the original three-dimensional patches are transformed into two-dimensional ones in order to be able to calculate position comparisons more performantly. The covariance matrix $\mathbf{C}_{XX}$ is optional and can only be filled by the patches. From the covariance matrix, the accuracy of the patches can be calculated, which depends on the measurement accuracy and the quality of the co-registration.

3.1 Registration

The novel approach to registering point clouds using the BIM model has already been published and validated in Gruner et al. 2022. The aim is to avoid the need of ground control points. The approach requires a (partially) existing BIM model in which the highly precise point cloud is to be registered. It is important to note that the further development took place within the commercial registration software *Scantra*. „From the perspective of the registration software, the digital building model (BIM) becomes nothing more than an additional TLS standpoint. The term virtual station is used to illustrate that perspective.“ (Gruner et al. 2022)

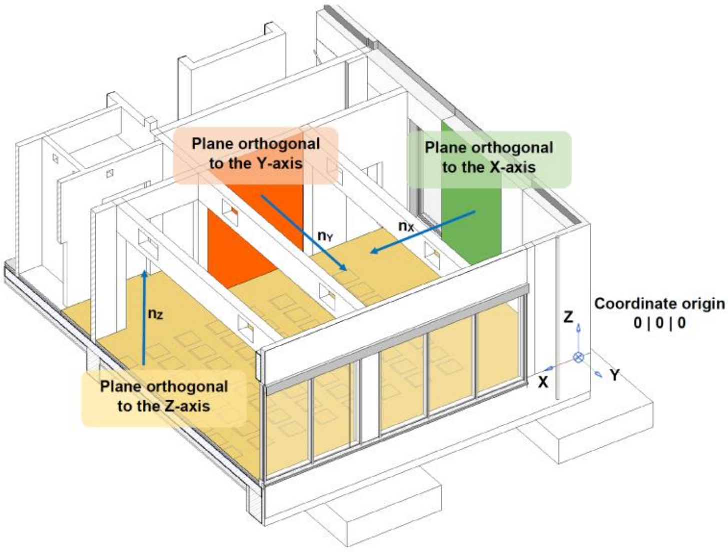

Figure 3: BIM model with 3 colored BIM faces, which are necessary at least for registration.

The required BIM planes (faces) can be extracted from IFC or Revit files and written to *Scantra's* database. Then, instead of always linking patches together, patches are linked to the "artificial" BIM planes. Figure 3Figure 1 depicts the minimum configuration that is necessary, but it is also possible to use several hundred BIM planes to improve accuracy and control.

3.2 Visibility analysis

The basis for the calculation of the construction progress with regard to the target variable object permanence is a visibility analysis. This allows to determine which faces of the BIM model would have been measurable at all with a certain measurement configuration. Algorithm, presented in Table 1Listing 1 describes the procedure for calculating this analysis.

Listing 1: Algorithm for finding visible faces

Algorithm for finding visible faces
procedure GETVISIBLEFACES (**S**, **F**, **stepsPerFullTurn**)
S ← set of all stations
F ← set of all faces
$\mathbf{F_v}$→ set of all visible faces
for $\mathbf{S_i}$ in **S** **do**
O ← getOctants(S_i)
for $\mathbf{O_i}$ in **O** **do**
$\mathbf{F_j}$ ← allocateFaces($\mathbf{O_i}$, **F**)
$\mathbf{B_j}$ ← calcOctBeamBundle($\mathbf{S_i}$, **stepsPerFullTurn**)
for $\mathbf{B_k^j}$ in $\mathbf{B_j}$ **do**
for $\mathbf{F_k}$ in **F** **do**
p ← pointOfIntersection($\mathbf{B_k^j}$, $\mathbf{F_k}$)
d ← distance(**p**, $\mathbf{S_i}$)
end for
$\mathbf{f_v}$ ← faceWithShortestDistance

```
            end for
        end for
    end for
    return F_V
end procedure
```

The visibility analysis is divided into 3 steps, the reading of the data, the ray-casting, and the output of visible faces. For performance reasons, octants were calculated around each station, to which faces are assigned, so that not every simulated laser beam has to be intersected with every face.

1. Reading the Faces from BIM and Patches from DB
2. Raycasting
    a. Determination of the step size
    b. Division of the space into octants and assignment of the faces
    c. only faces of the relevant octant whose normal vector is also oriented to the station.
    d. Intersection calculation Ray-Face
    e. Calculate the distance between scanner station and the point of intersection
3. Save face with shortest distance

The points of intersection as well as a simulated point cloud are saved at the end of the analysis. By visualizing this, the set step size of the rays can be evaluated and possibly refined.

3.3 Allocation of Scan patches and BIM patches

Due to the large number of possible patch-patch combinations, filtering and allocation must be carried out. In addition, this can exclude possible interfering objects from the construction site on which patches were also detected. The first step is to assign a threshold value for the maximum difference in distance **d** and another for the largest angular difference between the normal vectors. After this compliance check, the bounding boxes are buffered and checked for overlap. This filtering reduces the number of relevant face-patch pairs that can be further compared. At the end of this allocation, each BIM face has either no, one or more patches allocated to it.

3.4 Statistical hypothesis testing

In the next step, statistical hypothesis tests are intended to answer the question of whether the relevant pairs comply with the given construction tolerance. The distance between the face and the patch is considered. With the help of the standard deviation, a confidence interval can be calculated. The formula for calculating the orthogonal distance **a** from BIM polygon point to the TLS plane is:

$$a = \overrightarrow{\mathrm{n}^{\mathrm{BIM}}} \cdot \overrightarrow{\mathrm{p}^{\mathrm{TLS}}} + \mathrm{d}^{\mathrm{BIM}}$$

$$a = n_x{}^{BIM} \cdot p_x{}^{TLS} + n_y{}^{BIM} \cdot p_y{}^{TLS} + n_z{}^{BIM} \cdot p_z{}^{TLS} + d^{BIM}$$

The polygon points of a patch are used with the plane parameters $\vec{\mathbf{n}}$ and **d** of the BIM face. The known accuracy of the patches can be used to check whether the calculated distance is significant. For the hypothesis test, the standard deviation $\boldsymbol{\sigma_a}$ of **a** is required, which can be computed by means of error propagation. For the function **F**, the matrix must be determined with the help of partial derivatives.

$$C_{aa} = F \cdot C_{xx}^{p} \cdot F^T$$

$$F = \begin{bmatrix} \frac{\partial a^p}{\partial p_x^{TLS}} & \frac{\partial a^p}{\partial p_y^{TLS}} & \frac{\partial a^p}{\partial p_z^{TLS}} \end{bmatrix}$$

$$F = \begin{bmatrix} n_x^{BIM} & n_y^{BIM} & n_z^{BIM} \end{bmatrix}$$

$$\sigma_a = \sqrt{C_{aa}}$$

The test variable **a** is normally distributed and then compared with the normalized 99.5% quantile:

$$a \sim N(0,1)$$

$$z = \frac{a}{\sigma_a}$$

$$z_{0.995} = 2.6$$

$$z < z_{0.995}$$

After this statistical test has been passed, the verification can take place whether the distance is within the valid construction tolerance. Figure 4 shows the tolerance interval around the target value. The confidence interval around the actual value can move like a slider on the x axis.

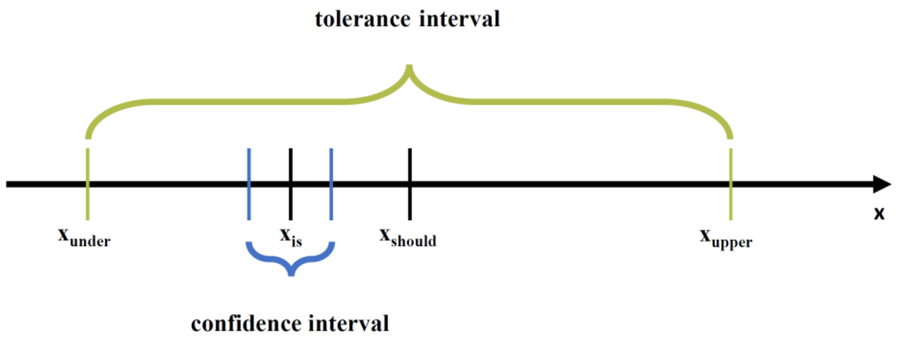

Figure 4: The position of these two intervals to each other must be tested.

The position is determined and there are 5 possible cases, which are listed in Table 2.

Table 2: Possible cases in the placement of the confidence interval in the tolerance interval

No.	Confidence interval is...	Compliance with the tolerance
1	smaller than x_{under}	no
2	located around x_{under}	uncertain
3	greater than x_{under} and smaller than x_{upper}	yes
4	located around x_{upper}	uncertain
5	greater than x_{upper}	no

All patches that satisfy the building tolerance are projected onto the face plane and clipped to it. This allows to calculate the percentage of a face that is covered by patches. The faces are classified according to these values and visualized accordingly.

3.5 Construction Tolerance

The construction tolerance can set by the user, by default it is 3 cm. This sensitive threshold value is subject to many engineering premises and has a strong influence on the test result.

3.6 Visualization and Reporting

The results can be saved directly as parameters of the components and visualized in BIM. It is also possible to create component lists with the corresponding analysis results. In addition, a comprehensive log is saved for more detailed information. A detailed protocol is generated which is structured according to BIM faces and contains:

- Non-measurable faces
- Measurable but actually not measured faces
- Measured faces
- Number of patches in evaluation box, number of patches with significant change, number of patches without significant change
- Number of patches outside tolerance range, number of patches uncertain, number of patches within tolerance range
- Listing of all patches for a face (a, σ_a, z, change (yes/no), construction tolerance (yes/uncertain/no), covered area)

Detailed protocol structured according to TLS patches contains:

- Number of faces (can also be 0, often 1, mostly > 1)
- Number of faces within/without deviation? H_0: $a = 0$, a, σ_a, z (yes/no)
- Number of faces within/without the tolerance (yes/uncertain/no)

The results of the intermediate steps can be exported as an OBJ-file at any time for quick visualization.

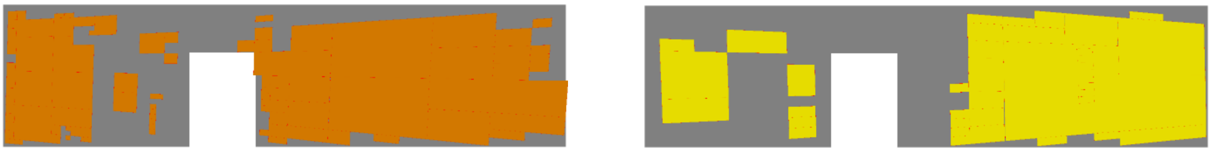

Figure 5: Visualization of the patches on a BIM face(grey) from 2 scanner stations

For example, Figure 6 visualizes the patches assigned to a BIM face.

4. EXPERIMENTAL VALIDATION

The new approach and software implementation was tested on a real BIM construction site. Two epochs were scanned and compared individually with the BIM model. The registration was carried out with the help of BIM planes and therefore did not require any control points. The registration result depends on the match between model and reality. It became clear that the height component of the Scan-BIM shift is less accurate than the positional components. The standard deviation of the adjusted horizonal translation parameters is less than 1 cm, but the Z component is up to 2 cm. The reason for this is the small number of horizontal faces and their variability due to the layered structure of the floor and the often suspended ceilings. Nevertheless, the analysis can be used for walls and their position because the vertical patches have a low standard deviation. The calculated distances **a** have a standard deviation $\boldsymbol{\sigma_a}$ of at least 3 mm.

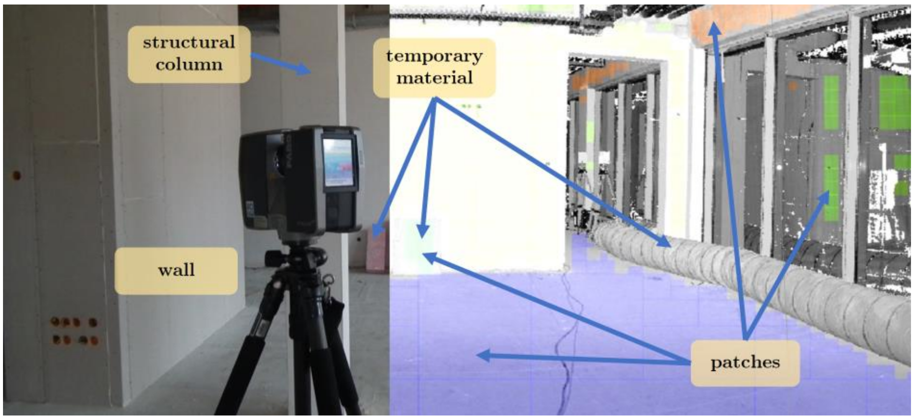

Figure 6: Transition from photo to plane-extracted point cloud

The legend for the used colors (figure 8) applies to all succeeding figures (figures 9-12):

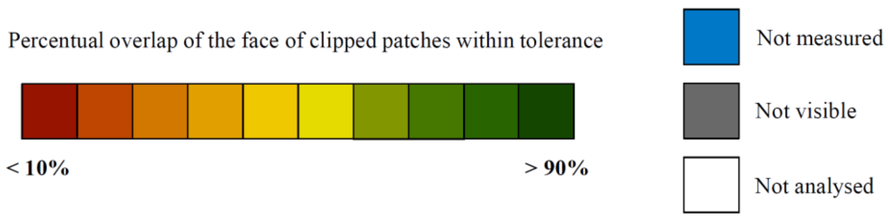

Figure 7: Legend of the colours to visualize the test results

Measured faces are colored according to the scale in Figure 7. Invisible faces are colored grey and visible faces that were not measured are colored blue.

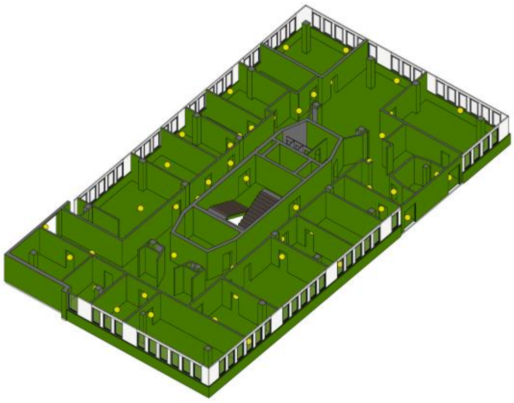

Figure 8: Result of the visibility analysis: Most BIM faces are scanned with >50% overlap (green)

There were a lot of temporary objects on the real construction site. These could be filtered out by assigning the patches to the faces. Nevertheless, visual occlusions are created by the disturbance objects. In addition, glass windows create mirrored false patches, as depicted on the right of Figure 6. The quantitative result of the epoch 0 and epoch 1 is shown in Table 3.

Table 3: Results of the analysis:

Field	Epoch 0	Epoch 1
patches	97092	31696
faces	1011	1011
not visible faces	538	551
visible faces that were not measured	231	361
visible faces that were measured	242	99
allocated patches	26445	12372

Epoch 0 represents the status before the conversion works. In epoch 1, most of the partition walls had been removed. From table 3 it can be seen that there is a very high number of patches and therefore the allocation is necessary because otherwise every patch would have to be tested with every face. The number of invisible faces is approximately the same, because this depends only on the stations.

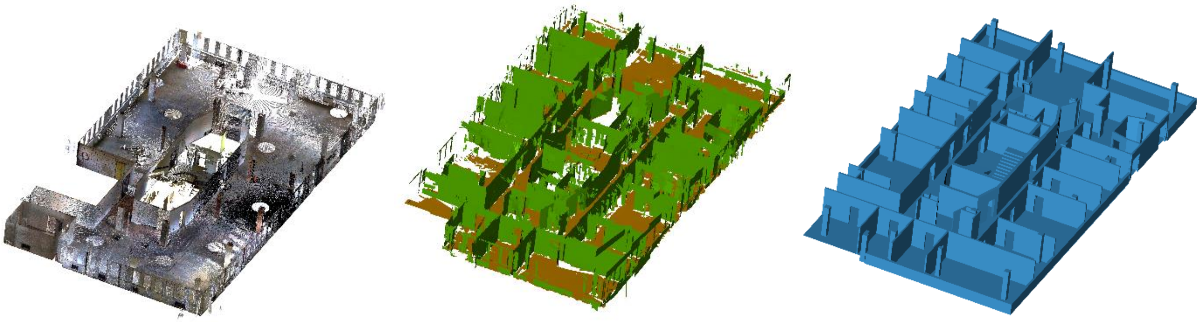

Figure 9: Processed data: colored point cloud (left), extracted patches from the point cloud (middle) and faces from the BIM model (right)

Figure 9 shows the point cloud on the left, the extracted patches from the point cloud in the middle and extracted faces from BIM on the right. As shown in figure 11, two epochs are compared to the given BIM model.

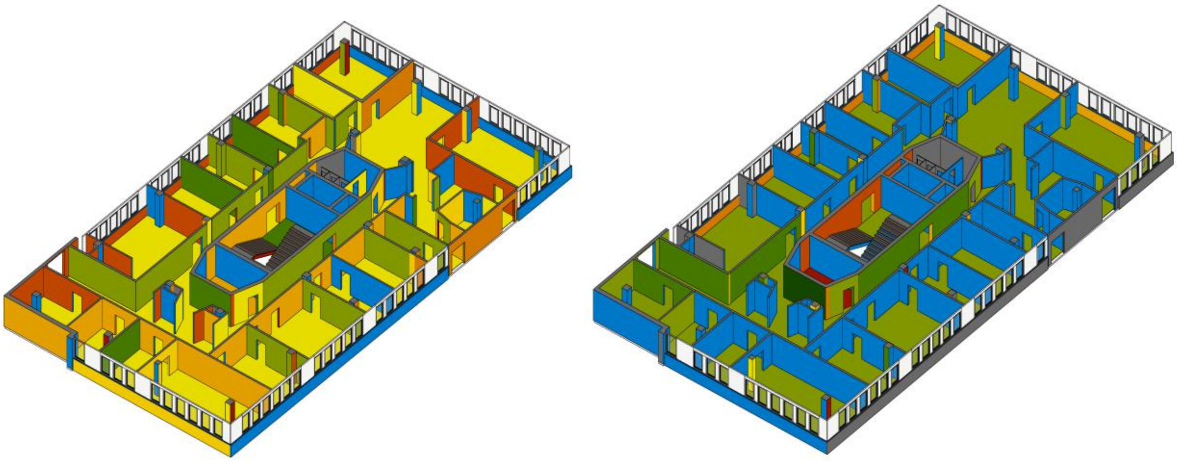

Figure 10: Result of the analysis of epoch 0 (left) and epoch 1 (right)

The test shows, that in epoch 0 (left) the walls and ceilings had been fully reduced to the shell, so that individual walls and the structural columns show significant deviations (red). To determine the progress of construction, the two epochs must be compared with each other. The measured and unmeasured faces of the two epochs are compared. This results in four possible states:

- unchanged existing (in figure colored green)
- demolished (in figure colored red)
- new built (in figure colored yellow)
- unchanged not existing (in figure colored grey)

Also the demolished walls had been automatically detected in epoch 1 (right)

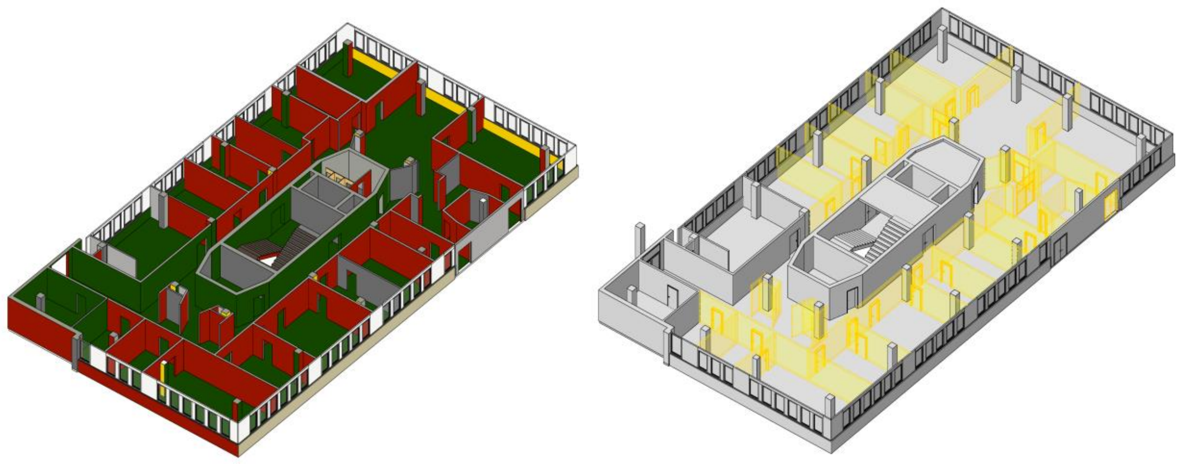

Figure 11: Comparison of two scanned epochs by patch analysis (left). The results (red) fit to the planned demolition in BIM (right)

Figure 12 shows how the algorithm analyzes the demolition of walls on site. The epoch comparison of two scans in the BIM software is visualized on the left. The red walls were measured by the screen in epoch 0, in epoch 1 these walls were actually no longer there. The right figure shows the demolition planning (yellow/transparent), modeled in the BIM software as phases. A comparison of the right and left figures shows a high level of agreement. All partition walls were removed, except for the central core and two rooms.

5. CONCLUSION

In this paper, a plane-based method for construction progress monitoring using a virtual building model was presented. By using planes instead of single points, the error budget could be included in the analysis. Construction progress is determined by computing orthogonal distances between assigned building and scan planes into a tolerance interval. The analysis only uses shell elements and it is fundamentally important that the BIM model depicts a realistic view of the construction. The innovative registration using planes from the BIM model has achieved sufficient accuracy in practice. By including the error budget, statistically significant analyses could be calculated. The defined target values, which are necessary for a comprehensive construction progress control, could be determined automatically in the practical example. In the future, the software is to be further developed so that not only distances but also possible misrotations of components can be detected and shown to the user. Furthermore, first software development steps have been taken to use a software-independent IFC file as a basis. Further research on the subject could also look at checking the deformation of building components.

6. ACKNOWLEDGEMENT

The research project "ProgressPatch" was funded by the German Federal Ministry for Economic Affairs and Energy. Grant No. 16KN057445.

REFERENCES

Bassier, Maarten; Vincke, Stan; Mattheuwsen, Lukas; Lima Hernandez, Roberto de; Derdaele, Jens; Vergauwen, Maarten (2019): Percentage of completion of in-situ cast concrete walls using point cloud data and BIM. In *Int. Arch. Photogramm. Remote Sens. Spatial Inf. Sci.* XLII-5/W2, pp. 21–28. DOI: 10.5194/isprs-archives-XLII-5-W2-21-2019.

Bermudez, Manuel E. (2012): A Mobile Field Diary System for Infrastructure Construction Project Inspections (Latin American and Caribbean Conference for Engineering and Technology, 10).

Besl, Paul J.; McKay, Neil D. (1992): Method for registration of 3-D shapes. In. Sensor Fusion IV: Control Paradigms and Data Structures: International Society for Optics and Photonics (1611), pp. 586–606. Available online at https://www.spiedigitallibrary.org/conference-proceedings-of-spie/1611/0000/method-for-registration-of-3-d-shapes/10.1117/12.57955.short.

Bosché, Frédéric (2010): Automated recognition of 3D CAD model objects in laser scans and calculation of as-built dimensions for dimensional compliance control in construction. In *Advanced Engineering Informatics* 24 (1), pp. 107–118. DOI: 10.1016/j.aei.2009.08.006.

Bosché, Frédéric; Ahmed, Mahmoud; Turkan, Yelda; Haas, Carl T.; Haas, Ralph (2015): The value of integrating Scan-to-BIM and Scan-vs-BIM techniques for construction monitoring using laser scanning and BIM: The case of cylindrical MEP components. In *Automation in Construction* 49, pp. 201–213. DOI: 10.1016/j.autcon.2014.05.014.

Gielsdorf, Frank; Rietdorf, Andreas; Gründig, Lothar (Eds.) (2004): A Concept for the Calibration of Terrestrial Laser Scanners. FIG Working Week. Greece, 22.05.2004-27.05.2004. Fédération Internationale des Géomètres.

Gruner, Felix; Romanschek, Enrico; Wujanz, Daniel; Clemen, Christian (2022): CO-REGISTRATION OF TLS POINT CLOUDS WITH SCAN-PATCHES AND BIM-FACES. In *Int. Arch. Photogramm. Remote Sens. Spatial Inf. Sci.* XLVI-5/W1-2022, pp. 109–114. DOI: 10.5194/isprs-archives-XLVI-5-W1-2022-109-2022.

Guo, Jingjing; Wang, Qian; Park, Jae-Hyuk (2020): Geometric quality inspection of prefabricated MEP modules with 3D laser scanning. In *Automation in Construction* 111, p. 103053. DOI: 10.1016/j.autcon.2019.103053.

Ibrahim, Y. M.; Lukins, T. C.; Zhang, X.; Trucco, E.; Kaka, A. P. (2009): Towards automated progress assessment of workpackage components in construction projects using computer vision. In *Advanced Engineering Informatics* 23 (1), pp. 93–103. DOI: 10.1016/j.aei.2008.07.002.

Kim, Changyoon; Kim, Byoungil; Kim, Hyoungkwan (2013): 4D CAD model updating using image processing-based construction progress monitoring. In *Automation in Construction* 35, pp. 44–52. DOI: 10.1016/j.autcon.2013.03.005.

Omar, Tarek; Nehdi, Moncef L. (2016): Data acquisition technologies for construction progress tracking. In *Automation in Construction* 70, pp. 143–155. DOI: 10.1016/j.autcon.2016.06.016.

Puri, Nisha; Turkan, Yelda (2020): Bridge construction progress monitoring using lidar and 4D design models. In *Automation in Construction* 109, p. 102961. DOI: 10.1016/j.autcon.2019.102961.

Rebolj, Danijel; Babič, Nenad Čuš; Magdič, Aleš; Podbreznik, Peter; Pšunder, Mirko (2008): Automated construction activity monitoring system. In *Advanced Engineering Informatics* 22 (4), pp. 493–503. DOI: 10.1016/j.aei.2008.06.002.

Rebolj, Danijel; Pučko, Zoran; Babič, Nenad Čuš; Bizjak, Marko; Mongus, Domen (2017): Point cloud quality requirements for Scan-vs-BIM based automated construction progress monitoring. In *Automation in Construction* 84, pp. 323–334. DOI: 10.1016/j.autcon.2017.09.021.

Rietdorf, Andreas (2005): Automatisierte Auswertung und Kalibrierung von scannenden Messsystemen mit tachymetrischem Messprinzip. With assistance of Technische Universität Berlin, Lothar Gründig.

Scott, Steve; Assadi, Sami (1997): Towards an electronic site diary. In *Information Technology Support for Construction Process Re-engineering*, pp. 349–358.

Stilla, Uwe; Xu, Yusheng (2023): Change detection of urban objects using 3D point clouds: A review. In *ISPRS Journal of Photogrammetry and Remote Sensing* 197, pp. 228–255. DOI: 10.1016/j.isprsjprs.2023.01.010.

Tuttas, Sebastian; Braun, Alexander; Borrmann, André; Stilla, Uwe (2017): Acquisition and Consecutive Registration of Photogrammetric Point Clouds for Construction Progress Monitoring Using a 4D BIM. In *PFG* 85 (1), pp. 3–15. DOI: 10.1007/s41064-016-0002-z.

Valero, Enrique; Adán, Antonio (2016): Integration of RFID with other technologies in construction. In *Measurement* 94, pp. 614–620. DOI: 10.1016/j.measurement.2016.08.037.

Wang, Lung-Chuang; Lin, Yu-Cheng; Lin, Pao H. (2007): Dynamic mobile RFID-based supply chain control and management system in construction. In *Advanced Engineering Informatics* 21 (4), pp. 377–390. DOI: 10.1016/j.aei.2006.09.003.

Wu, Yuhong; Kim, Hyoungkwan; Kim, Changyoon; Han, Seung H. (2010): Object Recognition in Construction-Site Images Using 3D CAD-Based Filtering. In *J. Comput. Civ. Eng.* 24 (1), pp. 56–64. DOI: 10.1061/(ASCE)0887-3801(2010)24:1(56).

Wujanz, Daniel (2012): Towards transparent quality measures in surface based registration processes: Effects of deformation onto commercial and scientific implementations (XXXIX-B5), pp. 251–256.

Wujanz, Daniel; Schaller, Sandro; Gielsdorf, Frank; Gründig, Lothar (2018): Plane-based registration of several thousand laser scans on standard hardware. In *Int. Arch. Photogramm. Remote Sens. Spatial Inf. Sci.* XLII-2, pp. 1207–1212. DOI: 10.5194/isprs-archives-XLII-2-1207-2018.

Xu, Yusheng; Stilla, Uwe (2021): Toward Building and Civil Infrastructure Reconstruction From Point Clouds: A Review on Data and Key Techniques. In *IEEE J. Sel. Top. Appl. Earth Observations Remote Sensing* 14, pp. 2857–2885. DOI: 10.1109/JSTARS.2021.3060568.

Yang, Jun; Park, Man-Woo; Vela, Patricio A.; Golparvar-Fard, Mani (2015): Construction performance monitoring via still images, time-lapse photos, and video streams: Now, tomorrow, and the future. In *Advanced Engineering Informatics* 29 (2), pp. 211–224. DOI: 10.1016/j.aei.2015.01.011.

CONTACTS

Felix Gruner | Enrico Romanschek | Christian Clemen
HTW Dresden
Friedrich-List-Platz 1
01069 Dresden
GERMANY
Tel. +49 351 462 3405
Email: felix.gruner2 | enrico.romanschek | christian.clemen | @htw-dresden.de
Website: https://www.htw-dresden.de/en/university/facultys/spatial-information

Daniel Wujanz
technet GmbH
Am Lehnshof 8
13467 Berlin – Germany
daniel.wujanz@technet-gmbh.com
Web site: https://www.technet-gmbh.com/en/products/scantra/